

A. Turlapov^{1,2} · J. Kinast¹ · B. Clancy¹ ·
Le Luo¹ · J. Joseph¹ · J. E. Thomas^{1,3}

Is a gas of strongly interacting atomic fermions a nearly perfect fluid?

XX.XX.2007

Keywords Fermi gas, superfluidity, quantum viscosity, strong interactions

Abstract We use all-optical methods to produce a highly-degenerate Fermi gas of spin-1/2 ${}^6\text{Li}$ atoms. A magnetic field tunes the gas near a collisional (Feshbach) resonance, producing strong interactions between spin-up and spin-down atoms. This atomic gas is a paradigm for strong interactions in nature, and provides tests of current quantum many-body calculational methods for diverse systems, including very high temperature superconductors, nuclear matter in neutron stars, and the quark-gluon plasma of the Big Bang. We have measured properties of a breathing mode over a wide range of temperatures. At temperatures both below and well above the superfluid transition, the frequency of the mode is nearly constant and very close to the hydrodynamic value. However, explaining both the frequency and the damping rate in the normal collisional regime has not been achieved. Our measurements of the damping rate as a function of the energy of the gas are used to estimate an upper bound on the viscosity. Using our new measurements of the entropy of the gas, we estimate the ratio of the shear viscosity to the entropy density, and compare the result with the lower bound for quantum viscosity recently predicted using string theory methods.

PACS numbers: 03.75.Ss, 32.80.Pj.

1 Introduction

Optically-trapped, strongly-interacting atomic Fermi gases^{1,2} provide a unique laboratory for testing nonperturbative many-body theories in a variety of fields, from neutron stars and nuclear matter^{3,4,5} to quark-gluon plasmas⁶ and high temperature superconductors⁷. In contrast to other Fermi systems, in atomic gases,

1: Department of Physics, Duke University, Durham, NC 27708-0305, USA

2: Current address: Institute of Applied Physics, Russian Academy of Sciences, 46 ul. Ulyanova, Nizhniy Novgorod, 603950, Russia

3: E-mail: jet@phy.duke.edu

one may tune at will the interactions^{8,9,10}, energy^{11,12}, and spin populations^{13,14}. The strong interactions are produced using a Fano – Feshbach resonance^{1,15,16}, where the scattering length for zero-energy s-wave collisions is large compared to the interparticle spacing.

In a strongly-interacting 50-50 mixture of spin-up and spin-down atoms, evidence of new, high-temperature superfluidity has been found in the studies of collective dynamics^{1,17,18,19} and confirmed by the observation of quantized vortex lattices²⁰. Microscopic properties of the superfluid have been probed by detecting pairs of Fermi atoms in projection experiments^{21,22}, radiofrequency spectroscopy experiments^{23,24}, and optical spectroscopy measurements of the order parameter²⁵. Measurements of the heat capacity¹¹, collective damping¹², and entropy²⁶ near resonance reveal transitions in behavior close to the temperature predicted for the onset of Fermi superfluidity. Despite the microkelvin range of temperatures, the phenomenon is referred to as “high-temperature superfluidity” because the transition temperature is a large fraction ($\simeq 30\%$) of the Fermi temperature.

Measurements of the physical properties of strongly interacting Fermi atoms are not limited to atomic physics and can be extended to other Fermi systems: Fermi gases near a broad Feshbach resonance exhibit universal interactions^{1,3,27} and universal thermodynamics^{28,29}, i. e. the properties of the gas do not depend on the details of the interaction potentials (as long as the potential range is small) and are identical to those of other resonantly-interacting Fermi systems. For example, in a uniform strongly interacting gas, the ground-state energy is a universal fraction, denoted $1 + \beta$, of the energy of a noninteracting gas at the same density^{1,27}. The universal energy relationship was originally explored theoretically in the context of nuclear matter^{3,4} and has later been measured using ultracold Fermi atoms^{1,8,10,14,30,31}.

The strongly-interacting atomic gas behaves as a fluid over a wide range of temperatures^{12,32}. In the lower temperature range, this hydrodynamic behavior is explained by superfluidity^{12,17}. At temperatures well above the superfluid transition, the observed hydrodynamic frequency and the measured damping rate are not consistent with a model of a collisional normal gas^{12,33,34}. The microscopic mechanism that provides hydrodynamic properties at high temperatures is an open question.

In this paper, we review the hydrodynamic properties of a strongly-interacting gas consisting of an equal mixture of spin-up and spin-down atoms. We also present model-independent data on hydrodynamic oscillations of the gas, i.e., the frequency and damping rate of the radial breathing mode¹² as a function of the energy. These results should be useful for future comparison with theoretical models.

The search for a fluid with the viscosity at the quantum minimum is another feature of our study of strongly-interacting atomic Fermi gases. On general grounds, Kovtun et al.³⁵, predicted that for any fluid the ratio of shear viscosity η to entropy density s is always $\geq \hbar/4\pi k_B$ (k_B is Boltzmann’s constant). For a resonantly-interacting atomic gas, we estimate the ratio η/s from previous measurements of damping¹² and entropy²⁶. We discuss whether the atomic gas can be used for testing the fundamental η/s limit.

2 Experimental system

The starting point of our experiments is a highly degenerate, strongly-interacting Fermi gas of ${}^6\text{Li}$. The cloud is prepared using evaporation of an optically-trapped, 50-50 mixture of spin-up/down states at 840 G, just above the center of a broad Feshbach resonance^{1,11,12,17,19}. To reduce the temperature, we do not employ a magnetic sweep from a molecular BEC, in contrast to several other groups^{18,22,36}. Instead, we evaporate directly in the strongly attractive regime, nearly on the Feshbach resonance¹.

During the forced evaporation, the depth of the CO_2 laser optical trap is reduced to a small fraction (0.002 – 0.0005) of its maximum value ($\simeq 700 \mu\text{K}$), and then recompressed to the final value, usually 4.6% of the maximum trap depth for the breathing mode experiments¹². From the trap frequencies measured at 4.6% of full trap depth, and corrected for anharmonicity, we obtain the trap aspect ratio $\lambda = \omega_z/\omega_\perp = 0.045$ ($\omega_\perp = \sqrt{\omega_x\omega_y}$) and the mean oscillation frequency $\bar{\omega} = (\omega_x\omega_y\omega_z)^{1/3} = 2\pi \times 589(5)$ Hz. The shape of the trap slightly departs from cylindrical symmetry: $\omega_x/\omega_y = 1.107(0.004)$. Typically, the total number of atoms after cooling is $N = 2.0(0.2) \times 10^5$. The corresponding Fermi energy $E_F = k_B T_F$ and Fermi temperature T_F at the trap center for a noninteracting gas are given by $T_F = (3N)^{1/3} \hbar \bar{\omega} / k_B \simeq 2.4 \mu\text{K}$ at 4.6% of the maximum trap depth. For these conditions, the coupling parameter of the strongly-interacting gas at $B = 840$ G is $k_F a \simeq -30.0$, where $\hbar k_F = \sqrt{2m k_B T_F}$ is the Fermi momentum, and $a = a(B)$ is the zero-energy scattering length estimated from the measurements of Bartenstein et al.³⁷.

This completes preparation of the gas at nearly the ground state. The energy of the gas is increased from the ground state value by abruptly releasing the cloud and then recapturing it after a short expansion time t_{heat} . During the expansion time, the total kinetic and interaction energy is conserved. When the trapping potential $U(\mathbf{x})$ is reinstated, the potential energy of the expanded gas is larger than that of the initially trapped gas, increasing the total energy by a known factor¹¹. After waiting for the cloud to reach equilibrium, the sample is ready for subsequent measurements. The energy is then directly measured in model-independent way from the mean square axial cloud size as described below.

3 The thermodynamic parameter: Energy or Temperature

Equilibrium thermodynamic properties of the trapped gas, as well as dynamical properties, can be measured as functions of the temperature T or of the total energy E_{tot} . Knowledge of one such variable completely determines the properties of a universal system with a known particle number N (provided the local density approximation is valid).

To date, two model-independent thermometry methods have been reported for a strongly-interacting gas. The thermometry method of the MIT group³⁸ is only applicable to imbalanced mixtures of spin-up and spin-down atoms and is based on fitting the non-interacting edge of the majority cloud by a Thomas-Fermi distribution with unconstrained temperature. The method of the Duke group is based on measuring the entropy as a function of energy, $S_{tot}(E_{tot})$ ²⁶. This method has

been reported for a balanced mixture of spin-up and spin-down fermions. Noting that $1/T = \partial S_{tot} / \partial E_{tot}$, it has been proposed that for known energy the temperature can be obtained by differentiating a fit to the $S_{tot}(E_{tot})$ data. In this method, however, it is necessary to parametrize the data.

The other two known thermometry methods are model dependent and rely on magnetic field sweeps between the molecular BEC or noninteracting gas regime and the strongly interacting regime^{23,39}. The temperature of the strongly interacting gas is then estimated from that measured in the BEC or noninteracting gas using a theoretical model of the entropy⁴⁰. The other thermometry method of the Duke group¹¹ is based on comparing the measured density distribution with an approximate model for the density profiles⁴¹.

A model-independent parametrization of the data is provided by measuring the energy of the trapped gas. In the universal regime, the energy per particle $E = E_{tot}/N$ can be easily measured because the trapped gas obeys the virial theorem³²:

$$\langle U(\mathbf{x}) \rangle = \frac{E}{2}, \quad (1)$$

where $U(\mathbf{x})$ is the harmonic trapping potential and $\langle U(\mathbf{x}) \rangle$ represents average potential energy per particle. This result is remarkable: Despite the complicated many-body strongly interacting ground state, the gas obeys the same virial theorem as a non-interacting Fermi gas. This theorem provides a simple model-independent energy measurement, just from the size of the cloud. In the local density approximation, with an isotropic pressure, it is easy to show from Eq. 1 that the energy per particle in a 50-50 mixture of two spin states in a harmonic trap is

$$E = 3m\omega_z^2 \langle z^2 \rangle, \quad (2)$$

where z is the axial direction of the cigar-shaped cloud. The energy can also be measured from the radial dimension of the expanded cloud in the hydrodynamic regime, where the expansion factor is known¹.

For the radial breathing mode near the Feshbach resonance, we present both the frequency and damping rate data as a function of energy per particle to provide model-independent results.

4 Hydrodynamic flow of a strongly interacting Fermi gas

Hydrodynamic flow was observed in the very first and simplest experiments with a strongly-interacting Fermi gas, where the gas was released from a cigar-shape trap¹. The signature of hydrodynamic flow was the anisotropic expansion of the cigar cloud into a disc, i.e. the flow was in the direction of the largest pressure gradient, inverting the aspect ratio after expansion.

In-trap hydrodynamics can be studied by observing the compression (breathing) mode of the gas^{9,12,17,18,19}. There are two distinct frequency regimes, for a hydrodynamic fluid and for a collisionless normal gas. In a cigar-shape trap with our parameters, for the radial mode, these frequencies are $\omega = 1.84 \omega_{\perp}$ and $\omega = 2.10 \omega_{\perp}$, respectively. In the universal gas, the hydrodynamic frequency has been predicted to stay the same at any temperature as long as the flow remains isentropic³².

In the experiment, the radial breathing mode is excited by releasing the cloud and recapturing the atoms after $25 \mu\text{s}$ (for 4.6% of the maximum trap depth). After the excitation, we let the cloud oscillate for a variable time t_{hold} , at the end of which the gas is released and imaged after $\simeq 1 \text{ ms}$ of expansion¹⁷. The snap-shots of the oscillating gas are shown in Fig. 1. The measured frequency

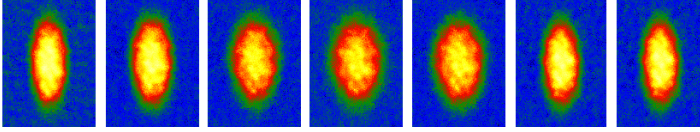


Fig. 1 Snap-shots of gas after oscillation for a variable time t_{hold} , followed by release and expansion for 1 ms. Each measurement is destructive. t_{hold} is increasing from left to right.

(Fig. 2) remains at the hydrodynamic value over the nominal temperature range $T = 0.12 - 1.1 T_F$ ¹², which corresponds to an energy range from nearly the ground state value $\simeq 0.5 E_F$ to $3.0 E_F$. The frequency stays far below the frequency of a

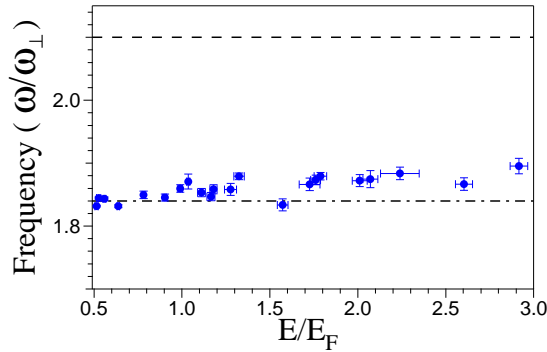


Fig. 2 Breathing mode in a strongly-interacting gas. Normalized frequency versus the normalized energy per particle. The superfluid phase transition is located at $E_c \simeq E_F$. The upper dotted line shows the frequency for a noninteracting gas.

non-interacting gas. No signatures of the superfluid transition are seen in the frequency dependence, but we can obtain several estimates of the critical energy from measurements of other thermodynamic quantities, such as the entropy and heat capacity. In these two quantities, a change in behavior is observed at $E_c = 0.94 E_F$ ($T = 0.29 T_F$) and $E_c = 0.85 E_F$ ($T = 0.27 T_F$), respectively. In Figure 3, we display the normalized damping rate $1/\omega_{\perp} \tau$ versus the energy. In contrast to the frequency, the damping rate exhibits interesting features. At $E_c = 1.01 E_F$ one observes a clear change in the damping versus energy dependence: The monotonic rise switches to flat dependence, which might be a signature of a phase transition.

In examining these features, it is appropriate to ask: What are the microscopic mechanisms that cause the gas to have hydrodynamic properties? Hydrodynamic behavior can appear via at least two mechanisms: (i) superfluidity and (ii) normal

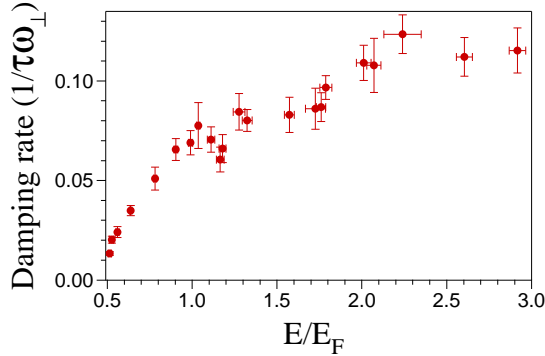


Fig. 3 Breathing mode in a strongly-interacting gas. Normalized damping versus the normalized energy per particle.

dynamics of atomic gas with large number of collisions. Below $E_c = 1.01 E_F$, the reduction in the damping rate as $T \rightarrow 0$ is consistent with superfluidity, and inconsistent with the scenario of a collisional normal gas^{12,17}. Above E_c , however, collisional dynamics of a normal atomic gas does not completely explain the observed behavior. For such a normal system, Bruun and Smith³⁴ found that hydrodynamic behavior is only possible at $T < 1.4 T_F$, i.e. only for temperatures where the collision rate is large enough. The highest observed damping rate $1/\tau = 0.12 \omega_\perp$ occurs for $E > 2.2 E_F$ and is consistent with predictions for a transition from hydrodynamic to collisionless behavior³⁴. However, the high damping rate is predicted to occur with a higher frequency, closer to $2.10 \omega_\perp$ ³⁴.

It is possible that above the phase transition, the dynamics is significantly affected by the presence of non-condensed pairs. The step in damping rate at about $E \simeq 2E_F$ might be due to pair-breaking since at this energy, the trap-averaged binding energy becomes smaller than $\hbar\omega$ ¹². A pseudogap formalism^{11,41} as well as the recent observation of the MIT group⁴² suggests that atoms can be paired at temperatures well above the phase transition.

5 Quantum viscosity

In a strongly interacting system Fermi gas, where the interparticle separation $l \propto 1/k_F$ sets the length scale, there is a natural unit of shear viscosity η which has dimension of momentum divided by cross section. The relevant momentum is the Fermi momentum, $\hbar k_F = \hbar/l$. The relevant area is determined by the unitarity-limited collision cross section $4\pi/k_F^2 \propto l^2$. Hence, $\eta \propto \hbar/l^3 = \hbar n$, where n is the local total density, so that

$$\eta = \alpha \hbar n. \quad (3)$$

Here, α is generally a dimensionless function of the local reduced temperature $T/T_F(n)$, where $T_F(n) \equiv \hbar^2(3\pi^2 n)^{2/3}/2mk_B$ is the local Fermi temperature. Eq. 3 has been discussed by Shuryak⁴³. We see that viscosity has a natural quantum scale, $\hbar n$. If the coefficient α is of order unity or smaller, we say that the system is in the quantum viscosity regime.

Using string theory methods, Kovtun et al., have shown that for a wide class of strongly interacting quantum fields, the ratio of the shear viscosity to the entropy density has a universal minimum value³⁵. The entropy density s has units of nk_B . Hence, in the ratio η/s the density cancels so that η/s has natural units of \hbar/k_B . The string theory prediction is

$$\frac{\eta}{s} \geq \frac{1}{4\pi} \frac{\hbar}{k_B}. \quad (4)$$

An important question is then how close a strongly interacting Fermi gas comes to the minimum quantum viscosity limit. Answering this question requires the determination of two physical quantities, shear viscosity and entropy density. To estimate the ratio η/s , we separately integrate the numerator and denominator over the trap volume. Then using $\int d^3\mathbf{x}n = N$, where N is the total number of atoms and $\int d^3\mathbf{x}s = S_{tot}$ is the total entropy, one obtains,

$$\frac{\eta}{s} \simeq \frac{\int d^3\mathbf{x}\eta}{\int d^3\mathbf{x}s} = \frac{\hbar}{k_B} \frac{\langle\alpha\rangle}{S/k_B}. \quad (5)$$

Here, $\langle\alpha\rangle \equiv (1/N) \int d^3\mathbf{x}n\alpha(\mathbf{x})$ is the trap average of the dimensionless universal function α that determines the shear viscosity according to Eq. 3 and $S = S_{tot}/N$ is the entropy per particle which has been measured as a function of energy²⁶.

We estimate $\langle\alpha\rangle(E)$ from the damping rate $1/\tau$ of the radial breathing mode, Fig. 3. If the damping rate arises from shear viscosity, then the value of $\langle\alpha\rangle$ is readily determined. Using the shear pressure tensor⁴⁴ in the hydrodynamic equations of motion for the radial breathing mode³², we easily obtain

$$\frac{1}{\tau\omega_{\perp}} = \frac{\hbar\omega_{\perp}}{E} \langle\alpha\rangle. \quad (6)$$

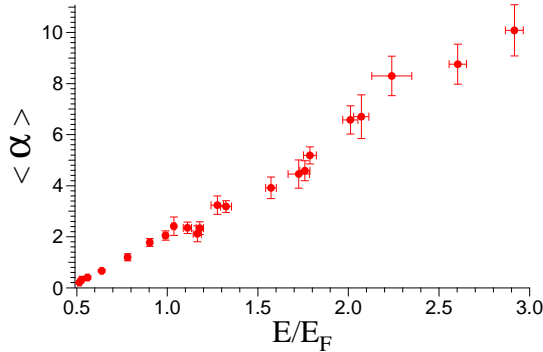


Fig. 4 Quantum viscosity in strongly-interacting Fermi gas. The local shear viscosity takes the form $\eta = \alpha \hbar n$. In the figure, $\langle\alpha\rangle$ is a trap-averaged value of the dimensionless parameter α .

We determine the energy per particle in a model independent way by exploiting the virial theorem, as discussed above^{26,32}. Using our measured damping ratios $1/(\tau\omega_{\perp})$ as a function of energy, we determine $\langle\alpha\rangle(E)$, as shown in Fig. 4.

Using the values of $\langle\alpha\rangle(E)$ from Fig. 4 and the measured entropy $S(E)$ from Ref.²⁶ in Eq. 5, we estimate the ratio of the viscosity to entropy density, as shown in Fig. 5. A similar plot has been given previously by Thomas Schäfer, based on our damping and entropy measurements⁴⁵. In the plot, note that $E_0 \simeq 0.5E_F$ is the ground state energy and E_F is the Fermi energy of a noninteracting gas at the trap center. The superfluid transition occurs near $E = E_F$, above which the gas is normal. For comparison, the estimated value for ${}^3\text{He}$ and ${}^4\text{He}$ near the λ -point is $\eta/s \simeq 0.7$. For a quark-gluon plasma, a current theoretical estimate⁴⁶ is $\eta/s = 0.16 - 0.24$.

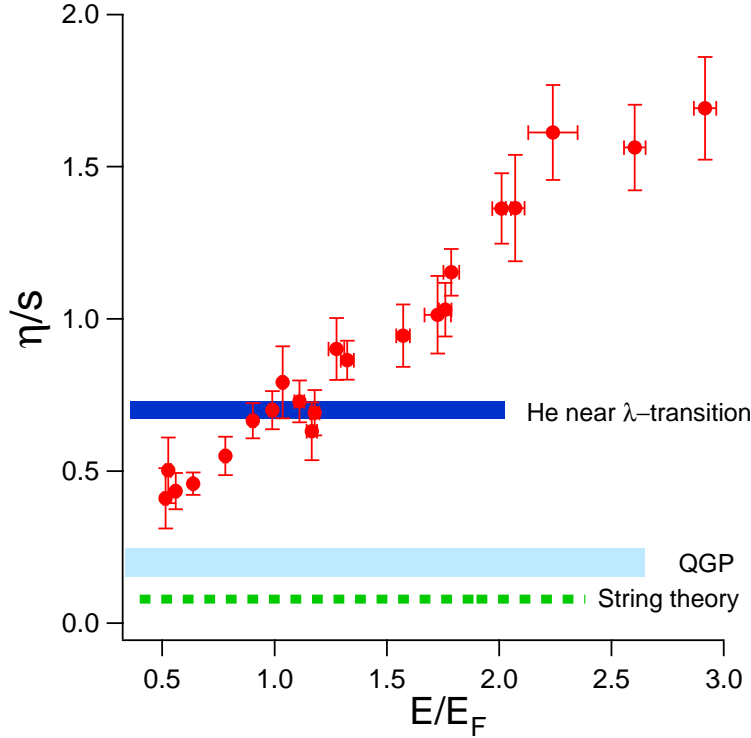


Fig. 5 Ratio of the shear viscosity η to the entropy density s for a strongly interacting Fermi gas as a function of energy E , red solid circles. The lower green dotted line shows the string theory prediction $1/(4\pi)$. The light blue bar shows the estimate for a quark-gluon plasma (QGP)⁴⁶, while the blue solid bar shows the estimate for ${}^3\text{He}$ and ${}^4\text{He}$, near the λ -point.

While our initial estimates for the η/s ratio place the strongly interacting Fermi gas in the quantum viscosity regime, a caveat for our result is that we have not proven that the damping arises from viscosity¹². Other sources of damping may contribute, for example Landau damping⁴⁷. Thus, the actual viscosity may be lower. Our data may not be determining the minimum viscosity, which may make a contribution that is smaller than the total measured damping rate.

6 Conclusion

We have explored the fluid properties of a strongly interacting Fermi gas. Measurements of the frequency and damping of the radial breathing mode as a function of energy provide model-independent data that indicate very low viscosity, fluid-like behavior over a wide range of energies covering both the superfluid and normal phases. The measured frequency agrees with the macroscopic model of universal isentropic hydrodynamics. The unitary collision dynamics that provides this fluid-like behavior well above the phase transition is not completely understood. Our estimate of the viscosity over entropy density ratio (η/s) places strongly interacting Fermi gases in the quantum viscosity regime.

Acknowledgements

This research has been supported by the Army Research Office and the National Science Foundation, the Physics for Exploration program of the National Aeronautics and Space Administration, and the Chemical Sciences, Geosciences and Biosciences Division of the Office of Basic Energy Sciences, Office of Science, U. S. Department of Energy.

References

1. K. M. O'Hara, S. L. Hemmer, M. E. Gehm, S. R. Granade, J. E. Thomas, *Science* **298**, 2179 (2002).
2. J. E. Thomas, M. E. Gehm, *Am. Scientist* **92**, 238 (2004).
3. H. Heiselberg, *Phys. Rev. A* **63**, 043606 (2001).
4. G. A. Baker, Jr., *Phys. Rev. C* **60**, 054311 (1999).
5. J. Carlson, S.-Y. Chang, V. R. Pandharipande, K. E. Schmidt, *Phys. Rev. Lett.* **91**, 050401 (2003).
6. P. F. Kolb, U. Heinz, *Quark Gluon Plasma 3* (World Scientific, 2003), p. 634.
7. Q. Chen, J. Stajic, S. Tan, K. Levin, *Phys. Rep.* **412**, 1 (2005).
8. M. Bartenstein, *et al.*, *Phys. Rev. Lett.* **92**, 120401 (2004).
9. A. Altmeyer, *et al.*, *Phys. Rev. Lett.* **98**, 040401 (2007).
10. J. Joseph, *et al.*, *Phys. Rev. Lett.* **98**, 170401 (2007).
11. J. Kinast, *et al.*, *Science* **307**, 1296 (2005).
12. J. Kinast, A. Turlapov, J. E. Thomas, *Phys. Rev. Lett.* **94**, 170404 (2005).
13. M. W. Zwierlein, A. Schirotzek, C. H. Schunck, W. Ketterle, *Science* **311**, 492 (2006).
14. G. B. Partridge, W. Li, R. I. Kamar, Y. Liao, R. G. Hulet, *Science* **311**, 503 (2006).
15. M. Houbiers, *et al.*, *Phys. Rev. A* **56**, 4864 (1997).
16. M. Houbiers, H. T. C. Stoof, W. I. McAlexander, R. G. Hulet, *Phys. Rev. A* **57**, R1497 (1998).
17. J. Kinast, S. L. Hemmer, M. E. Gehm, A. Turlapov, J. E. Thomas, *Phys. Rev. Lett.* **92**, 150402 (2004).
18. M. Bartenstein, *et al.*, *Phys. Rev. Lett.* **92**, 203201 (2004).
19. J. Kinast, A. Turlapov, J. E. Thomas, *Phys. Rev. A* **70**, 051401(R) (2004).

-
20. M. Zwierlein, J. Abo-Shaeer, A. Schirotzek, C. Schunck, W. Ketterle, *Nature* **435**, 1047 (2005).
 21. C. A. Regal, M. Greiner, D. S. Jin, *Phys. Rev. Lett.* **92**, 040403 (2004).
 22. M. W. Zwierlein, *et al.*, *Phys. Rev. Lett.* **92**, 120403 (2004).
 23. C. Chin, *et al.*, *Science* **305**, 1128 (2004).
 24. M. Greiner, C. A. Regal, D. S. Jin, *Phys. Rev. Lett.* **94**, 070403 (2005).
 25. G. B. Partridge, K. E. Strecker, R. I. Kamar, M. W. Jack, R. G. Hulet, *Phys. Rev. Lett.* **95**, 020404 (2005).
 26. L. Luo, B. Clancy, J. Joseph, J. Kinast, J. E. Thomas, *Phys. Rev. Lett.* **98**, 080402 (2007).
 27. M. E. Gehm, S. L. Hemmer, S. R. Granade, K. M. O'Hara, J. E. Thomas, *Phys. Rev. A* **68**, 011401(R) (2003).
 28. T.-L. Ho, *Phys. Rev. Lett.* **92**, 090402 (2004).
 29. H. Hu, P. D. Drummond, X.-J. Liu, *Nature Physics* **3**, 469 (2007).
 30. T. Bourdel, *et al.*, *Phys. Rev. Lett.* **91**, 020402 (2003).
 31. C. A. Regal, M. Greiner, S. Giorgini, M. Holland, D. S. Jin, *Phys. Rev. Lett.* **95**, 250404 (2005).
 32. J. E. Thomas, A. Turlapov, J. Kinast, *Phys. Rev. Lett.* **95**, 120402 (2005).
 33. P. Massignan, G. M. Bruun, H. Smith, *Phys. Rev. A* **71**, 033607 (2005).
 34. G. M. Bruun, H. Smith, *Phys. Rev. A* **75**, 043612 (2007).
 35. P. K. Kovtun, D. T. Son, A. O. Starinets, *Phys. Rev. Lett.* **94**, 111601 (2005).
 36. T. Bourdel, *et al.*, *Phys. Rev. Lett.* **93**, 050401 (2004).
 37. M. Bartenstein, *et al.*, *Phys. Rev. Lett.* **94**, 103201 (2005).
 38. M. W. Zwierlein, C. H. Schunck, A. Schirotzek, W. Ketterle, *Nature* **442**, 54 (2006).
 39. Q. Chen, C. A. Regal, D. S. Jin, K. Levin, *Phys. Rev. A* **74**, 011601(R) (2005).
 40. Q. Chen, J. Stajic, K. Levin, *Phys. Rev. Lett.* **95**, 260405 (2005).
 41. J. Stajic, Q. Chen, K. Levin, *Phys. Rev. Lett.* **94**, 060401 (2005).
 42. C. H. Schunck, Y. Shin, A. Schirotzek, M. W. Zwierlein, W. Ketterle, *Science* **316**, 867 (2007).
 43. E. Shuryak, *Prog. Part. Nucl. Phys.* **53**, 273 (2004).
 44. L. D. Landau, E. M. Lifshitz, *Fluid Mechanics* (Pergamon Press, New York, 1975).
 45. T. Schafer, The shear viscosity to entropy density ratio of trapped fermions in the unitary limit (2007). ArXiv:cond-mat/0701251.
 46. Steffen Bass, Duke University, private communication.
 47. P. O. Fedichev, G. V. Shlyapnikov, J. T. M. Walraven, *Phys. Rev. Lett.* **80**, 2269 (1998).